Rapid adiabatic gating for capacitively coupled quantum dot hybrid qubits without barrier control

A. A. Setser and J. P. Kestner

Department of Physics, University of Maryland Baltimore County, Baltimore, Maryland 21250, USA

We theoretically examine the capacitive coupling between two quantum dot hybrid qubits, each consisting of three electrons in a double quantum dot, as a function of the energy detuning of the double dot potentials. We show that a shaped detuning pulse can produce a two-qubit maximally entangling operation in ~50 ns without having to simultaneously change tunnel couplings. Simulations of the entangling operation in the presence of experimentally realistic charge noise yield two-qubit fidelities over 90%.

I. INTRODUCTION

Spin qubits in semiconductor quantum dots are attractive building blocks for quantum computers due to their small size and potential scalability. Single-spin qubits are a simple design in which single-electron spin states are used as the logical basis for computation [1]. These spin qubits have been realized experimentally in both one-qubit and two-qubit exchange-coupled settings [2–4]. Singlet-triplet qubits are another common type of spin qubit, where the logical basis is formed by singlet and triplet spin states [5,6]. Capacitive coupling is an attractive choice for two-qubit operations in singlet-triplet systems, due to the relatively simple experimental implementation and lack of leakage. Two-qubit entangling gates in these systems have been discussed theoretically [7–10] and recently demonstrated experimentally [11,12]. Typical gate times for capacitively coupled singlet-triplet qubits are on the order of hundreds of nanoseconds, making them generally susceptible to low-frequency charge noise unless special measures are taken [13]. A more recent type of spin qubit is the so-called hybrid qubit, which is encoded in the total spin state of three electrons in a double quantum dot, which allows for fully electrical control [14]. In that setting, capacitively coupled two-qubit gates are predicted to be shorter than typical entangling gates for singlet-triplet qubits [15].

In this paper, we examine adiabatic gates between strictly capacitively coupled hybrid qubits within the two-qubit logical subspace. This is a different situation than in Refs. [15,16], which permitted tunneling between qubits and considered diabatic gates. By setting the exchange interactions between qubits to zero in our case, the number of possible leakage states is reduced, typically leading to leakage errors significantly smaller than in Refs. [15,16]. The chargelike character of the hybrid qubit at small detunings gives rise to a large coupling strength while the spinlike character at large detunings effectively turns off the interaction between qubits, and recently Ref. [17] has shown that adiabatic pulses in the detuning can be used to perform entangling gates. Our work differs from Ref. [17] in two ways: (i) Ref. [17] considers simple sinusoidal ramp shapes, whereas we allow for shaped pulses of the detuning, and (ii) Ref. [17] allows different

detunings for each qubit and/or simultaneous control over the tunnel couplings, whereas we restrict to only symmetric detuning control.

By choosing an optimal pulse shape for the detuning, we show that two-qubit entangling operations can be performed in under 50 ns while maintaining adiabaticity. We then show that these short gate times give rise to qubits that are naturally robust against realistic charge noise, giving fidelities over 90%. This performance is comparable to the results obtained by Ref. [17] with an alternate approach.

II. MODEL

A single hybrid qubit consists of three electrons in a double quantum dot (DQD). For a system of two hybrid qubits, each DQD confines the three electrons in the lowest two valley states of each dot. The first and second qubits are, respectively, centered at positions $\pm R$ with respect to the origin, giving a total separation of $2R$. Each quantum well of a single DQD is centered at $\pm a$ with respect to the center of the DQD.

We consider states with spin $S = 1/2$ and $S_z = -1/2$. The possible spin states can be written as $|\cdot S\rangle, |\cdot T\rangle, |S\cdot\rangle$, and $|T\cdot\rangle$, where $|\cdot S\rangle = |\downarrow\rangle|S\rangle, |\cdot T\rangle = \sqrt{\frac{1}{3}}|\downarrow\rangle|T_0\rangle - \sqrt{\frac{2}{3}}|\uparrow\rangle|T_-\rangle, |S\cdot\rangle = |S\rangle|\downarrow\rangle$, and $|T\cdot\rangle = \sqrt{\frac{1}{3}}|T_0\rangle|\downarrow\rangle - \sqrt{\frac{2}{3}}|T_-\rangle|\uparrow\rangle$. The singlet, unpolarized triplet, and polarized triplet states are, respectively, represented by $|S\rangle, |T_0\rangle$, and $|T_-\rangle$. In this notation, $|\cdot S\rangle$ and $|\cdot T\rangle$ lie in a $(1, 2)$ configuration, while $|S\cdot\rangle$ and $|T\cdot\rangle$ lie in a $(2, 1)$ configuration. Depending on which direction the double well is biased, either $|\cdot T\rangle$ or $|T\cdot\rangle$ is a high-energy state and can be neglected. In the basis of the remaining low-energy states (either $\{|\cdot S\rangle, |\cdot T\rangle, |S\cdot\rangle\}$ or $\{|S\cdot\rangle, |T\cdot\rangle, |\cdot S\rangle\}$), the Hamiltonian for the ith qubit is given by [18],

$$H_i = \begin{pmatrix} -\frac{\varepsilon_i}{2} & 0 & \Delta_1^{(i)} \\ 0 & -\frac{\varepsilon_i}{2} + E_{ST}^{(i)} & \Delta_2^{(i)} \\ \Delta_1^{(i)} & \Delta_2^{(i)} & \frac{\varepsilon_i}{2} \end{pmatrix}, \quad (1)$$

where ε_i is the detuning (i.e., the energy difference between the two wells) of the ith qubit, and $E_{ST}^{(i)}$ is the singlet-triplet

energy splitting of two-spin states in a single well of the ith qubit. Given that typical fitted values for E_{ST} are significantly smaller than the orbital splitting in this reduced Hilbert space approximation [19], we assume that the singlet-triplet spin states of a single well occupy different valleys, rather than different orbitals. $\Delta_1^{(i)}$ represents the $|\cdot S\rangle \leftrightarrow |S\cdot\rangle$ transition for the ith qubit and $\Delta_2^{(i)}$ represents the $|\cdot T\rangle \leftrightarrow |S\cdot\rangle$ or $|T\cdot\rangle \leftrightarrow |\cdot S\rangle$ transition for the ith qubit. A $|\cdot S\rangle \leftrightarrow |\cdot T\rangle$ or $|S\cdot\rangle \leftrightarrow |T\cdot\rangle$ transition is not allowed, since these states occupy different valleys.

Assuming the confining potential is parabolic around the minimum of each well, the lowest two electronic wave functions can then be approximated by the valley-state wave functions given in Ref. [20]. Essentially, the single-particle basis orbitals have a harmonic ground-state envelope with an additional phase factor that distinguishes between valleys. We use the Hund-Mulliken approximation (or, equivalently, a heavily truncated configuration-interaction approach), in which the Hamiltonian is expanded using these noninteracting orbitals, keeping only the lowest orbitals of each dot, which is a standard method for quantum dot systems [21–23]. It is important to note that the harmonic orbitals are simply the basis we expand in, and are not the exact orbitals that include the effects of electron-electron interactions in their shape. Rather, the electron-electron interactions are accounted for through a set of two-electron Coulomb integrals included in the Hamiltonian. While we consider only the lowest orbitals of each dot, there are also nonvanishing matrix elements, which couple ground harmonic orbitals to excited harmonic orbitals. In Sec. III, we show that, for experimentally realistic parameters, these matrix elements are negligible on the energy scales we consider, thereby allowing the Hund-Mulliken approximation to be valid.

Assuming the barrier between qubits is high enough that interqubit tunneling is negligible and the interaction between qubits is purely capacitive, we can incorporate the two-qubit interaction through a set of two-electron Coulomb integrals. There are three terms, corresponding to the three possible types of overall charge configurations: $(2, 1, 1, 2)$, $(1, 2, 2, 1)$, or $(1, 2, 1, 2)/(2, 1, 2, 1)$, assuming identical double wells, where (i, j, k, l) denotes the charge configuration (i, j) of the first qubit and (k, l) of the second qubit. In general, $(1, 2, 1, 2)$ and $(2, 1, 2, 1)$ charge configurations may not be completely equivalent due to asymmetry in the DQDs, but this will not qualitatively change the results. So, for the sake of simplicity, we focus on the symmetric case. Then the spatial distribution of the three charge configurations leads to three unique Coulomb interactions, which provides a nonzero energy difference between two-qubit states in separate charge configurations. The charge configuration of a low-energy eigenstate is a detuning-dependent mixture of the three types of overall charge configurations, and hence the detuning provides a means of controlling the interqubit interaction energy.

Each well must contain at least one electron, i.e., four of the six total electrons must be in a $(1, 1, 1, 1)$ charge configuration. The two leftover electrons can reside in any two unique wells, giving total charge configurations of $(1, 2, 2, 1)$, $(2, 1, 1, 2)$, or $(2, 1, 2, 1)/(1, 2, 1, 2)$. Since it is the two leftover electrons, which allow the different charge configurations to be distinguished, we can effectively ignore the interaction
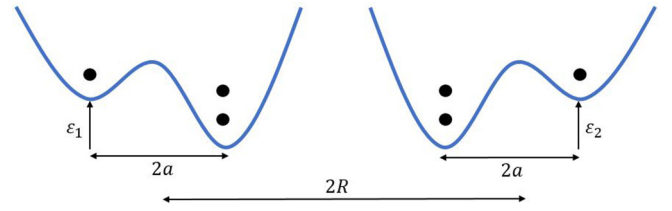

FIG. 1. Schematic of two DQDs separated by a distance $2R$, each with interdot distance $2a$. The potential of the first (second) qubit is centered at $-R$ $(+R)$. The detuning parameter ε_i is positive for both qubits and corresponds to a raising of the left well of the first qubit by ε_1 and a raising of the right well of the second qubit by ε_2.

due to the four electrons in the $(1, 1, 1, 1)$ configuration. Therefore, we need only consider Coulomb integrals for electrons in the configurations $(1, 0, 0, 1)$, $(0, 1, 1, 0)$, or $(1, 0, 1, 0)/(0, 1, 0, 1)$, which we denote, respectively, by V_f, V_n, V_m, i.e., far, near, and medium interactions. Since the direct Coulomb integral between valley-state wave functions centered at positions $\mathbf{r}_1$ and $\mathbf{r}_2$ simplifies to a direct Coulomb integral between ground-state harmonic wave functions centered at $\mathbf{r}_1$ and $\mathbf{r}_2$, the interaction terms are given by,

$$
\begin{aligned}
V_f &= \langle \phi_{-R-a}\phi_{+R+a}|\mathcal{C}|\phi_{-R-a}\phi_{+R+a}\rangle, \\
V_m &= \langle \phi_{-R-a}\phi_{+R-a}|\mathcal{C}|\phi_{-R-a}\phi_{+R-a}\rangle, \\
V_n &= \langle \phi_{-R+a}\phi_{+R-a}|\mathcal{C}|\phi_{-R+a}\phi_{+R-a}\rangle,
\end{aligned} \tag{2}
$$

where the general integral, $\langle \phi_{R_i}\phi_{R_k}|\mathcal{C}|\phi_{R_j}\phi_{R_l}\rangle$, is presented in Appendix B.

Tuning the quantum dots so that the low-energy basis states of the first and second qubits are, respectively, given by $\{|\cdot S\rangle, |\cdot T\rangle, |S\cdot\rangle\}$ and $\{|S\cdot\rangle, |T\cdot\rangle, |\cdot S\rangle\}$ (i.e., raising the energy of the left well of the left qubit and the right well of the right qubit), allows for a majority of the first and second qubit's states to lie respectively in the $(1, 2)$ and $(2, 1)$ charge configurations. This gives the largest number of near interactions, and hence the strongest coupling between qubits. With this convention, the detuning of both qubits is positive. A picture of the potential is shown in Fig. 1 for clarity. Summing the single-qubit Hamiltonians and including an interaction term, the two-qubit Hamiltonian is given as,

$$
H = H_1 \otimes I + I \otimes H_2 + H_{\text{int}}. \tag{3}
$$

Assuming the two-qubit basis is a Kronecker product of the single-qubit basis, the interaction Hamiltonian from the direct Coulomb coupling is given by $H_{\text{int}} = \text{diag}(V_n, V_n, V_m, V_n, V_n, V_n, V_m, V_m, V_f)$ (see Appendix A).

III. EFFECTIVE HAMILTONIAN

We form the effective Hamiltonian by restricting the evolution to the four lowest-energy states. The effective Hamiltonian in this subspace can be written in the basis of detuning-dependent instantaneous eigenstates as $H_{\text{eff}} = \text{diag}(E_1, E_2, E_3, E_4)$, where E_n is the nth smallest eigenvalue of the full Hamiltonian. In terms of the $SU(4)$ generators, we can also write

$$
H_{\text{eff}} = J_{ZI}\sigma_{ZI} + J_{ZZ}\sigma_{ZZ} + J_{IZ}\sigma_{IZ}, \tag{4}
$$

up to a constant term, where $\sigma_{ij} \equiv \sigma_i \otimes \sigma_j$, $J_{IZ} = 1/4(E_1 - E_2 + E_3 - E_4)$, $J_{ZI} = 1/4(E_1 + E_2 - E_3 - E_4)$, and $J_{ZZ} = 1/4(E_1 - E_2 - E_3 + E_4)$. As long as the detuning is changed adiabatically, no transitions between adiabatic eigenstates are induced. Local rotations about the Z axis are induced by J_{ZI} and J_{IZ}, while J_{ZZ} generates entanglement. Analytical expressions in terms of the Schrieffer-Wolff approximation are sometimes useful, but we are interested in the small-detuning regime where J_{ZZ} is large, and a perturbative form of H_{eff} is not valid; we therefore simply diagonalize the full 9×9 Hamiltonian numerically.

Matching typical silicon-based single-qubit experiments for hybrid qubits, we take an effective electron mass of $0.2m_0$ (m_0 is the electron rest mass), a dielectric constant of $\kappa = 11.7\epsilon_0$, a confinement energy of $\hbar\omega = 0.38$ meV (giving a Bohr radius of roughly 31 nm), and an interdot distance of $2a = 135$ nm [19]. We choose energy splittings and tunnel couplings of $E_{ST}^{(1)} = 52$ μeV, $E_{ST}^{(2)} = 47$ μeV, $\Delta_1^{(i)} = 0.64 \times E_{ST}^{(i)}$, and $\Delta_2^{(i)} = 0.58 \times E_{ST}^{(i)}$, which minimizes the effect of charge noise on the single qubit terms, J_{IZ} and J_{ZI} [17]. The interqubit distance is taken arbitrarily to be $2R = 8a \approx 543$ nm, which is similar in scale to non-capacitively coupled two-qubit silicon devices [3]. The Coulomb interaction terms are then $V_f = 181$ μeV, $V_m = 227$ μeV, and $V_n = 303$ μeV.

It should be noted that the 9×9 Hamiltonian implicitly assumes that only the lowest orbital can be populated. In general, there may be orbital excitations as well. Matrix elements, which couple the 9×9 Hamiltonian to these higher-energy terms can be shifted into the 9×9 Hamiltonian and treated perturbatively using the Schrieffer-Wolff transformation [14,24,25]. The nth-order perturbation term will go like $t^{n+1}/(\Delta U)^n$, where t is the transition rate to the higher-energy states and ΔU is the energy gap between the high-energy states and low-energy states. Since the transition rate is related to the movement of an electron into an excited orbital within a single well, it is approximated by the Coulomb integral $\langle \phi_{R_i} \phi_{R_j} | \mathcal{C} | \phi_{R_k} \widetilde{\phi}_{R_l} \rangle \approx 0.1$ μeV, where $\widetilde{\phi}_{R_m}$ denotes an orbital excitation centered at R_m, and R_i, R_j, R_k, and R_l are assigned the same numeric value (see Appendix B). Assuming $\Delta U \sim \hbar\omega = 0.38$ meV, the largest of the perturbative terms will be approximately 50 peV, which is more than an order of magnitude smaller than the minimum value of J_{ZZ} we consider [see Fig. 2(a)]. Under these assumptions, the 9×9 Hamiltonian accurately approximates the total Hilbert space.

Figure 2(b) shows the effect of the detuning on the effective coupling strength, where we set $\varepsilon_1 = \varepsilon_2 = \varepsilon$ for simplicity. Note that it is not the Coulomb energy itself that is directly relevant, but the energy difference between eigenstates. At large detunings, the four low-energy eigenstates making up the effective Hamiltonian are all roughly in $(1, 2, 2, 1)$ charge configurations. The energy difference between low-energy eigenstates due to the Coulomb interaction will be 0 since all eigenstates are in the same charge configuration, effectively giving $J_{ZZ} = 0$. At small detunings, the low-energy eigenstates will be mixtures of $(1, 2, 2, 1)$, $(2, 1, 1, 2)$, and $(1, 2, 1, 2)$ configurations. The low-energy eigenstates will then have a nonzero energy difference due to the Coulomb interaction. While the Coulomb interactions V_n, V_m, and V_f are all on the same order of magnitude, it is the energy
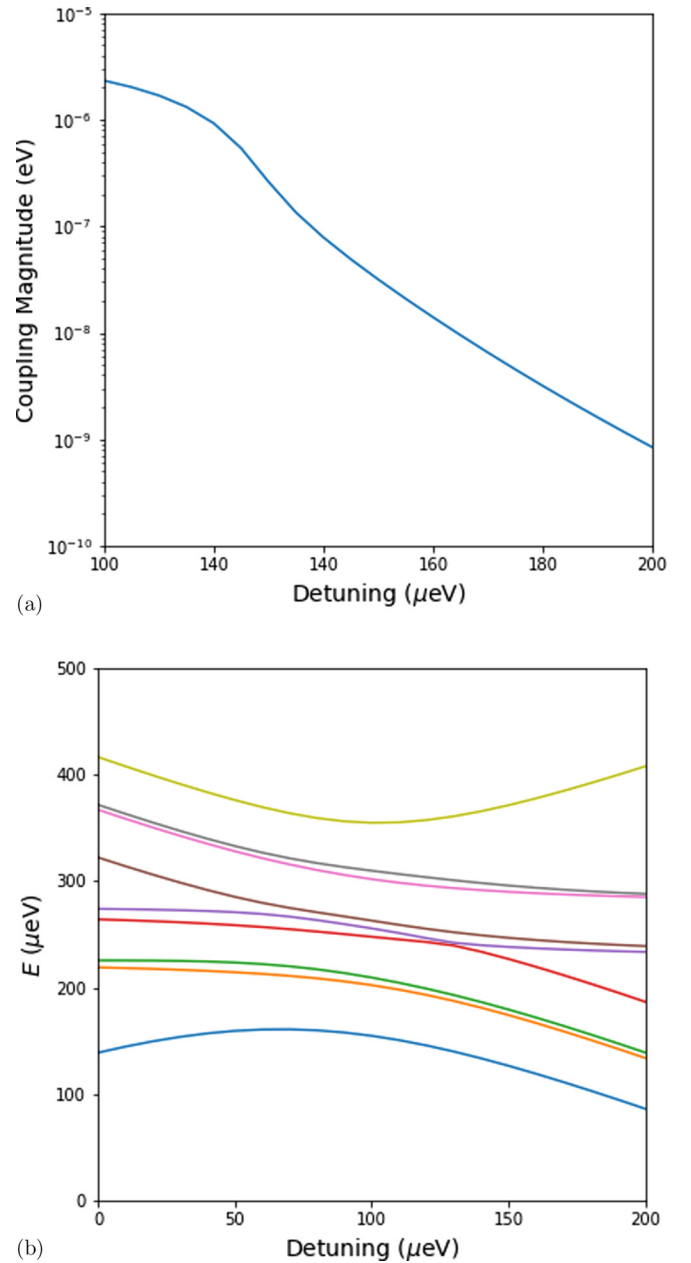

(a)

(b)

FIG. 2. (a) Semilog plot of the magnitude of the coupling term, J_{ZZ}, with $\varepsilon_1 = \varepsilon_2 = \varepsilon$, as a function of detuning. (b) The spectrum of the Hamiltonian assuming $\varepsilon_1 = \varepsilon_2 = \varepsilon$. At large detunings, the four lowest-energy levels (the logical subspace) are approximately parallel, signifying a coupling close to zero. As the detuning decreases, the logical subspace approaches the leakage space, causing an increased interaction.

differences between eigenstates, which change by several orders of magnitude.

The effect of any imperfections leading to nonidentical double wells is a slight shift in the value of the coupling, but the behavior is qualitatively unchanged. For example, if the difference in Coulomb interaction between electrons in a $(2, 1, 2, 1)$ configuration and $(1, 2, 1, 2)$ configuration is equal to 4 μeV, corresponding to, e.g., an imperfection causing intradot distances to differ by 5 nm, then the shift
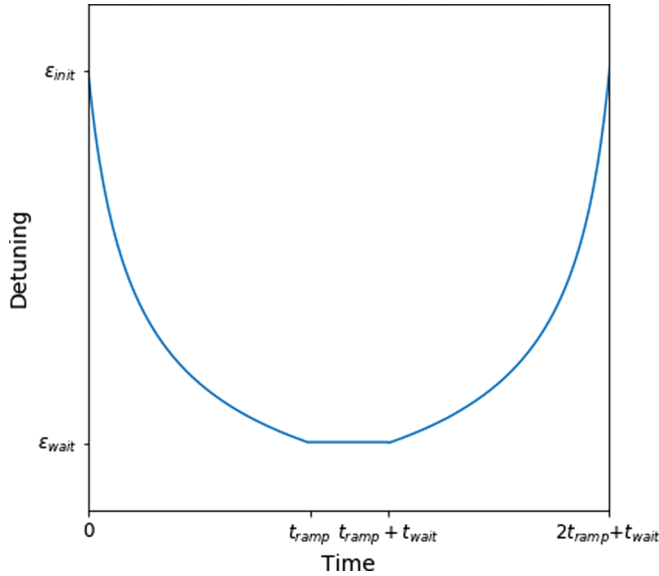
FIG. 3. An example of the total pulse. The detuning is lowered from $\varepsilon_{\text{init}}$ to $\varepsilon_{\text{wait}}$ over a time t_{ramp}. It is held at this point for a time t_{wait}, before being raised back to $\varepsilon_{\text{init}}$ over a time t_{ramp}. Here, $\alpha/\hbar = 79.0$, $t_{\text{ramp}} = 8.0$ ns, $t_{\text{wait}} = 2.9$ ns, $\varepsilon_{\text{init}} = 200$ μeV, and $\varepsilon_{\text{wait}} = 145$ μeV.

in coupling, ΔJ_{ZZ}, would be perturbed by between 65 neV around $\varepsilon = 100$ μeV and 0.4 neV around $\varepsilon = 200$ μeV.

IV. ADIABATIC RAMP

Both qubits are typically parked at an idle position at large detuning where the interaction is negligible, which we denote by $\varepsilon_{\text{init}}$. The two logical states of each qubit are defined as the lowest two eigenstates at that detuning. In order to perform an entangling operation, we adiabatically lower the detuning over a time t_{ramp} to a strongly interacting detuning $\varepsilon_{\text{wait}}$ where the qubits are held for a time t_{wait}. The detuning is then adiabatically returned back to $\varepsilon_{\text{init}}$. Thus, at the end of the pulse, minimal population has been transferred, and the qubits have picked up a nonlocal state-dependent phase.

We set $\varepsilon_{\text{init}} = 200$ μeV, so that the coupling is approximately 0 at the beginning and end of the ramp. As seen in Fig. 3, an avoided crossing between the logical subspace and leakage space occurs roughly around $\varepsilon = 130$ μeV. Choosing a value of $\varepsilon_{\text{wait}}$ below this point will require a long ramp time in order for the adiabatic approximation to be satisfied. For this reason, we restrict ourselves to $\varepsilon_{\text{wait}} \geqslant 130$ μeV.

Given that the coupling increases quickly as the detuning approaches the avoided crossing, it is useful to choose a pulse such that $\dot{\varepsilon}$ decreases as $\varepsilon \to \varepsilon_{\text{wait}}$. This ensures that the detuning will vary quickly when the gap between the logical and leakage space is large, and will vary slowly as the gap shrinks, minimizing nonadiabatic population loss into the leakage space. Such a pulse can be found as the numerical solution to the differential equation,

$$\dot{\varepsilon}(t) = \frac{1}{\alpha}[\Delta E(\varepsilon)]^2, \quad \varepsilon(0) = \varepsilon_{\text{init}}, \quad t \in [0, t_{\text{ramp}}], \quad (5)$$

where $\Delta E(\varepsilon)$ is the detuning-dependent energy difference between the fourth and fifth adiabatic eigenstates, α is an arbitrary scaling factor, which allows for control over the

ramp time, and t_{ramp} is defined via $\varepsilon(t_{\text{ramp}}) = \varepsilon_{\text{wait}}$ [26]. The detuning is swept back to its initial value via the time-reversed ramp shape. An example pulse shape is shown in Fig. 3.

This pulse shape is motivated by the Landau-Zener formula, which states that nonadiabatic transitions between the highest-lying eigenstate in the logical basis, ψ_4, and the lowest-lying eigenstate in the leakage space, ψ_5, are suppressed to first order when [27]

$$P = \int_0^{t_{\text{ramp}}} e^{i\Delta E t} V \, dt \ll 1, \quad (6)$$

where V is the coupling between states given by $i\langle\psi_4|\dot{\psi}_5\rangle$, which is equivalent to $i\langle\psi_4|\dot{H}|\psi_5\rangle/\Delta E$. Setting $P \ll 1$ is then loosely equivalent to setting $|V| \ll |\Delta E|$, which is true when $\langle\psi_4|\dot{H}|\psi_5\rangle \ll (\Delta E)^2$. This can also be written as $\langle\psi_4|\partial_\varepsilon H|\psi_5\rangle/\alpha \ll 1$, where α is defined as in Eq. (5). We note that the factor $\langle\psi_4|\partial_\varepsilon H|\psi_5\rangle$ can be dropped, since it is of order unity and does not significantly impact the inequality. This is known as the local adiabatic approach [26,28,29].

In the noise-free, adiabatic approximation, the ideal evolution operator is

$$\widetilde{U}_\theta = \exp\left[-i\int_0^{t_{\text{wait}}+2t_{\text{ramp}}} dt H_{\text{eff}}/\hbar\right], \quad (7)$$

where, for a given ramp time, the wait time is chosen such that the nonlocal phase acquired over the duration of the pulse is the desired angle, $\theta = \int_0^{t_{\text{wait}}+2t_{\text{ramp}}} dt J_{ZZ}/\hbar$. For a realistic simulation of the two-qubit operations, we can also consider the effects of noise on the qubits. The effects of charge noise on the qubits are modeled by random static perturbations in the detuning drawn from a Gaussian distribution with an experimentally measured standard deviation of $\sigma = 4.4$ μeV [30], i.e., $\varepsilon_i(t) \to \varepsilon(t) + \delta\varepsilon_i$, with $\delta\varepsilon_i$ independent of time and unique for each qubit. In addition, finite ramp times contribute nonadiabatic leakage. Thus, to obtain the actual evolution, when targeting a nonlocal phase θ, we numerically solve Schrödinger's equation for the full 9×9 Hamiltonian, using the ODEINT package available in SCIPY [31]. Note that we use the predetermined value of t_{wait} found from Eq. (7). This gives the full evolution operator, which includes the effects of charge noise as well as leakage. We then project the full evolution operator onto the lowest four eigenstates of the full Hamiltonian at $\varepsilon = \varepsilon_{\text{init}}$ (i.e., the logical basis) to get the effective (nonunitary) evolution operator, U_θ.

To target a maximally entangling operation, we choose $\theta = \pi/4$ so that the operation is locally equivalent to $\exp[-i\pi\sigma_{ZZ}/4]$. Note that this is sufficient, along with local rotations, to form a universal gate set. The fidelity between the noisy and noise-free evolution operators, $F(U_{\pi/4}, \widetilde{U}_{\pi/4})$, is calculated using the two-qubit fidelity defined in Ref. [32],

$$F(U_1, U_2) = \frac{1}{16}\left(4 + \frac{1}{5}\sum_{i,j\in\{I,X,Y,Z\}} \text{tr}(U_1\sigma_{ij}U_1^\dagger U_2\sigma_{ij}U_2^\dagger)\right), \quad (8)$$

averaged over 500 noise realizations.

The choice of α (thus, t_{ramp}) is arbitrary. Increasing the value of α serves to increase the ramp time, thus reducing errors due to leakage. Errors due to charge noise can be

suppressed by considering the Hamiltonian in the adiabatic frame, Eq. (4). The effect of charge noise on the terms in the Hamiltonian can be quantified by $\partial J_{ZZ}/\partial\varepsilon$, $\partial J_{IZ}/\partial\varepsilon$, and $\partial J_{ZI}/\partial\varepsilon$, which are all on the same order of magnitude. Fluctuations in these terms can be suppressed by interweaving applications of specific single-qubit operations in between applications of the noisy two-qubit operation. Specifically, J_{IZ} and J_{ZI} fluctuations can be suppressed completely with the sequence,

$$U_{\text{corrected}}(\pi/4) = U_{\pi/8}\sigma_{XX}U_{\pi/8}\sigma_{XX}, \qquad (9)$$

where σ_{XX} is a local π rotation about σ_X on both qubits. Note that while σ_{XX} is a two-qubit operation, it describes two single-qubit operations being performed simultaneously, and is nonentangling. Assuming essentially instantaneous single-qubit operations relative to the two-qubit gate times and negligible infidelities, we again numerically characterize the full evolution operator as before, except that now the Schrödinger equation is solved for a pulse, which is raised and lowered twice, with a nonlocal phase of $\pi/8$ accumulating over each pulse. It should also be noted that the second application of σ_{XX} is not necessary for error correction and does not affect the entangling power of the final operation. It simply adjusts the local part of the evolution to make the final operation equal to $U_{\pi/4}$. If local rotation errors are a concern, one could leave out the second application of σ_{XX}. Then, since the local operations have already been realized with fidelities above 99% [30], one might expect the corrected two-qubit gate fidelities we report to be lowered by at most 2% and even less if the local operations are improved. However, any more elaborate pulse sequences that involve a larger number of local operations may introduce more error than they correct. The fidelity $F(U_{\text{corrected}}, \widetilde{U}_{\pi/4})$ versus ramp time is shown in Fig. 4.

Optimizing over $\varepsilon_{\text{wait}}$, we found that the largest fidelity over all values of t_{ramp} was produced at approximately $\varepsilon_{\text{wait}} = 145\ \mu$eV, which is the value we use in the plot. For the simple uncorrected operation, we achieve a maximum fidelity of approximately 87.8% at $t_{\text{ramp}} = 5.3$ ns. For the corrected operation, we achieve a maximum fidelity of approximately 94.3% at $t_{\text{ramp}} = 4.3$ ns.

Sub-ns ramp times have low fidelity, due to large adiabatic errors close to 25% and 50% for the uncorrected and corrected operations, respectively. Increasing the ramp time quickly lowers errors due to nonadiabaticity below 1%, which is negligible compared to the errors due to charge noise. After errors due to nonadiabaticity become negligible, the fidelity remains roughly constant, rather than quickly becoming suppressed as the ramp time increases, as one would expect. The nonlocal phase, θ, can be split into the phase acquired over the ramping times when $t \in [0, t_{\text{ramp}}] \cup [t_{\text{ramp}} + t_{\text{wait}}, 2t_{\text{ramp}} + t_{\text{wait}}]$, and the phase acquired over the waiting time when $t \in [t_{\text{ramp}}, t_{\text{ramp}} + t_{\text{wait}}]$, which we denote, respectively, by θ_{ramp} and θ_{wait}. As t_{ramp} increases, θ_{ramp} also increases. Since $\theta_{\text{ramp}} + \theta_{\text{wait}} = \theta$, θ_{wait} must decrease as θ_{ramp} grows, meaning that as the ramp time increases, the wait time decreases. Thus, the total gate time is roughly constant just beyond the first few points for both lines.

For the uncorrected operation, a sharp drop in fidelity is seen around 10 ns. At this point, the nonlocal phase acquired by ramping up and immediately down (i.e., $t_{\text{wait}} = 0$) is larger
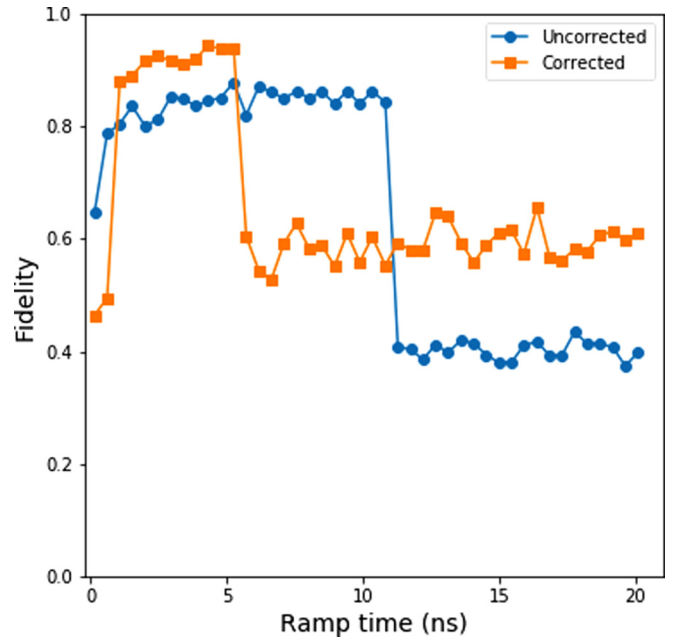

FIG. 4. Fidelity of the effective evolution operator versus ramp time, for both the corrected and uncorrected sequences, at $\varepsilon_{\text{wait}} = 145\ \mu$eV. t_{wait} is chosen at each point so that the noisy and noise-free operations in the logical subspace are locally equivalent to U_{target}.

than $\pi/4$. Regardless of the choice of t_{wait}, the nonlocal phase acquired by the evolution operator will be larger than $\pi/4$. Since the evolution operator is periodic in θ, we must then choose t_{wait} so that $\theta = \pi/4 + 2\pi$, leading to t_{wait} close to 80 ns, which is more than double the wait time required for smaller ramp times. The overall longer gate times lead to lower fidelities due to charge noise. A similar effect is also seen in the fidelity of the corrected operation.

This is comparable to the performance of Ref. [17], which uses a similar model, but a slightly different scheme. Rather than choosing the form of the ramp function to minimize nonadiabatic errors, Ref. [17] considers a sine-squared ramp for experimental simplicity and numerically optimizes simultaneous detuning and tunneling pulses, leading to a maximum fidelity around 90%.

V. CONCLUSION

We have shown that the Coulomb interaction between two hybrid qubits leads to a significant coupling strength within the logical subspace. Adjustment of the individual detunings allows for control over the charge configurations of the individual qubits, and hence the overall coupling strength. We have shown that this controllability allows for fast entangling operations to be performed in less than 50 ns.

By carefully choosing the detuning pulse shape and using known single-qubit error-correcting sequences, we have shown that fidelities over 90% can be achieved in the presence of realistic charge noise values, without changing tunnel couplings. Further increase in fidelity at the same noise levels would require going through a narrow avoided crossing in the energy eigenstates to access stronger couplings but while maintaining adiabaticity. This suggests the necessity of some

sort of shortcut-to-adiabaticity driving protocol, with full optimization on the detuning pulse shape simultaneous with tunnel coupling control, similar to the analysis in Ref. [17] but with less restriction on the allowed pulse shapes, in order to further improve the fidelity.

APPENDIX A: TWO-QUBIT HAMILTONIAN

For completeness, we present the two-qubit Hamiltonian given by Eq. (3) in the main text. The full matrix is given by

$$
H = \begin{pmatrix}
E_0 & 0 & \Delta_1^{(2)} & 0 & 0 & 0 & \Delta_1^{(1)} & 0 & 0 \\
0 & E_1 & \Delta_2^{(2)} & 0 & 0 & 0 & 0 & \Delta_1^{(1)} & 0 \\
\Delta_1^{(2)} & \Delta_2^{(2)} & E_2 & 0 & 0 & 0 & 0 & 0 & \Delta_1^{(1)} \\
0 & 0 & 0 & E_3 & 0 & \Delta_1^{(2)} & \Delta_2^{(1)} & 0 & 0 \\
0 & 0 & 0 & 0 & E_4 & \Delta_2^{(2)} & 0 & \Delta_2^{(1)} & 0 \\
0 & 0 & 0 & \Delta_1^{(2)} & \Delta_2^{(2)} & E_5 & 0 & 0 & \Delta_2^{(1)} \\
\Delta_1^{(1)} & 0 & 0 & \Delta_2^{(1)} & 0 & 0 & E_6 & 0 & \Delta_1^{(2)} \\
0 & \Delta_1^{(1)} & 0 & 0 & \Delta_2^{(1)} & 0 & 0 & E_7 & \Delta_2^{(2)} \\
0 & 0 & \Delta_1^{(1)} & 0 & 0 & \Delta_2^{(1)} & \Delta_1^{(2)} & \Delta_2^{(2)} & E_8
\end{pmatrix},
\tag{A1}
$$

where

$$
E_0 = V_n - \frac{\varepsilon_1}{2} - \frac{\varepsilon_2}{2}
\tag{A2}
$$

$$
E_1 = E_{ST}^{(2)} + V_n - \frac{\varepsilon_1}{2} - \frac{\varepsilon_2}{2}
\tag{A3}
$$

$$
E_2 = V_m - \frac{\varepsilon_1}{2} + \frac{\varepsilon_2}{2}
\tag{A4}
$$

$$
E_3 = E_{ST}^{(1)} + V_n - \frac{\varepsilon_1}{2} - \frac{\varepsilon_2}{2}
\tag{A5}
$$

$$
E_4 = E_{ST}^{(1)} + E_{ST}^{(2)} + V_n - \frac{\varepsilon_1}{2} - \frac{\varepsilon_2}{2}
\tag{A6}
$$

$$
E_5 = E_{ST}^{(1)} + V_m - \frac{\varepsilon_1}{2} + \frac{\varepsilon_2}{2}
\tag{A7}
$$

$$
E_6 = V_m + \frac{\varepsilon_1}{2} - \frac{\varepsilon_2}{2}
\tag{A8}
$$

$$
E_7 = E_{ST}^{(2)} + V_m + \frac{\varepsilon_1}{2} - \frac{\varepsilon_2}{2}
\tag{A9}
$$

$$
E_8 = V_f + \frac{\varepsilon_1}{2} + \frac{\varepsilon_2}{2}.
\tag{A10}
$$

APPENDIX B: TWO-ELECTRON COULOMB INTEGRALS

The general two-electron Coulomb integral between ground-state harmonic wave functions is given in Ref. [33] as,

$$
\langle \phi_{R_i} \phi_{R_k} | \mathcal{C} | \phi_{R_j} \phi_{R_l} \rangle = \frac{e^2}{4\pi\kappa} \sqrt{\frac{\pi}{2}} \frac{1}{a_B} \exp\left[-\frac{1}{4a_B^2}((R_i - R_j)^2 + (R_k - R_l)^2) \right]
$$
$$
\times \exp\left[-\frac{1}{16a_B^2}(R_i + R_j - R_k - R_l)^2 \right] I_0\left[\frac{1}{16a_B^2}(R_i + R_j - R_k - R_l)^2 \right],
\tag{B1}
$$

where I_0 is the zeroth-order modified Bessel function of the first kind, a_B is the effective Bohr radius, κ is the effective dielectric constant, and R_m is the distance from the center of the two DQDs to the center of the respective electron's wave function.

We are also interested in evaluating terms, which involve the interchange of electrons between different orbitals, such as $\langle \phi_{R_i} \phi_{R_k} | \mathcal{C} | \phi_{R_j} \widetilde{\phi}_{R_l} \rangle$, where $\widetilde{\phi}_{R_m}$ denotes an orbital excitation centered at R_m. This integral can be evaluated by noting that $\widetilde{\phi}_{R_m} = \sqrt{2} a_B \partial \phi_{R_m} / \partial R_m$. Using this relationship in $\langle \phi_{R_i} \phi_{R_k} | \mathcal{C} | \phi_{R_j} \widetilde{\phi}_{R_l} \rangle$ and noting that the integral is with respect to the spatial coordinates

of the wave functions, independent of R_m, the derivative can be pulled out of the integral, giving,

$$\langle \phi_{R_i}\phi_{R_k}|\mathcal{C}|\phi_{R_j}\widetilde{\phi}_{R_l}\rangle = \sqrt{2}a_B\frac{\partial}{\partial R_l}\langle \phi_{R_i}\phi_{R_k}|\mathcal{C}|\phi_{R_j}\phi_{R_l}\rangle, \tag{B2}$$

where the integral on the right-hand side is given by Eq. (B1).

[1] D. Loss and D. P. DiVincenzo, Phys. Rev. A **57**, 120 (1998).

[2] J. J. Pla, K. Y. Tan, J. P. Dehollain, W. H. Lim, J. J. L. Morton, D. N. Jamieson, A. S. Dzurak, and A. Morello, Nature (London) **489**, 541 (2012).

[3] M. Veldhorst, C. H. Yang, J. C. C. Hwang, W. Huang, J. P. Dehollain, J. T. Muhonen, S. Simmons, A. Laucht, F. E. Hudson, K. M. Itoh, A. Morello, and A. S. Dzurak, Nature **526**, 410 (2015).

[4] T. F. Watson, S. G. J. Philips, E. Kawakami, D. R. Ward, P. Scarlino, M. Veldhorst, D. E. Savage, M. G. Lagally, M. Friesen, S. N. Coppersmith, M. A. Eriksson, and L. M. K. Vandersypen, Nature **555**, 633 (2015).

[5] J. R. Petta, A. C. Johnson, J. M. Taylor, E. A. Laird, A. Yacoby, M. D. Lukin, C. M. Marcus, M. P. Hanson, and A. C. Gossard, Science **309**, 2180 (2005).

[6] H. Bluhm, S. Foletti, I. Neder, M. Rudner, D. Mahalu, V. Umansky, and A. Yacoby, Nature Phys. **7**, 109 (2011).

[7] D. Stepanenko and G. Burkard, Phys. Rev. B **75**, 085324 (2007).

[8] G. Ramon and X. Hu, Phys. Rev. B **81**, 045304 (2010).

[9] G. Ramon, Phys. Rev. B **84**, 155329 (2011).

[10] F. A. Calderon-Vargas and J. P. Kestner, Phys. Rev. B **97**, 125311 (2018).

[11] J. M. Nichol, L. A. Orona, S. P. Harvey, S. Fallahi, G. C. Gardner, M. J. Manfra, and A. Yacoby, npj Quantum Information **3**, 3 (2017).

[12] M. D. Shulman, O. E. Dial, S. P. Harvey, H. Bluhm, V. Umansky, and A. Yacoby, Science **336**, 202 (2012).

[13] R. K. L. Colmenar and J. P. Kestner, Phys. Rev. A **99**, 012347 (2019).

[14] Z. Shi, C. B. Simmons, J. R. Prance, J. K. Gamble, T. S. Koh, Y.-P. Shim, X. Hu, D. E. Savage, M. G. Lagally, M. A. Eriksson, M. Friesen, and S. N. Coppersmith, Phys. Rev. Lett. **108**, 140503 (2012).

[15] S. Mehl, arXiv:1507.03425.

[16] S. Mehl, Phys. Rev. B **91**, 035430 (2015).

[17] A. Frees, S. Mehl, J. K. Gamble, M. Friesen, and S. N. Coppersmith, arXiv:1812.03177.

[18] T. S. Koh, J. K. Gamble, M. Friesen, M. A. Eriksson, and S. N. Coppersmith, Phys. Rev. Lett. **109**, 250503 (2012).

[19] J. C. Abadillo-Uriel, B. Thorgrimsson, D. Kim, L. W. Smith, C. B. Simmons, D. R. Ward, R. H. Foote, J. Corrigan, D. E. Savage, M. G. Lagally, M. J. Calderón, S. N. Coppersmith, M. A. Eriksson, and M. Friesen, Phys. Rev. B **98**, 165438 (2018).

[20] D. Culcer, L. Cywiński, Q. Li, X. Hu, and S. Das Sarma, Phys. Rev. B **82**, 155312 (2010).

[21] G. Burkard, D. Loss, and D. P. DiVincenzo, Phys. Rev. B **59**, 2070 (1999).

[22] X. Hu and S. Das Sarma, Phys. Rev. A **61**, 062301 (2000).

[23] Q. Li, Ł. Cywiński, D. Culcer, X. Hu, and S. Das Sarma, Phys. Rev. B **81**, 085313 (2010).

[24] R. Winkler, *Spin-Orbit Coupling Effects in Two-Dimensional Electron and Hole Systems* (Springer, Berlin, 2003).

[25] S. Bravyi, D. P. DiVincenzo, and D. Loss, Ann. Phys. (NY) **326**, 2793 (2011).

[26] P. Richerme, C. Senko, J. Smith, A. Lee, S. Korenblit, and C. Monroe, Phys. Rev. A **88**, 012334 (2013).

[27] C. Wittig, J. Phys. Chem. B **109**, 8428 (2005).

[28] S. Martínez-Garaot, A. Ruschhaupt, J. Gillet, T. Busch, and J. G. Muga, Phys. Rev. A **92**, 043406 (2015).

[29] J. Roland and N. J. Cerf, Phys. Rev. A **65**, 042308 (2002).

[30] B. Thorgrimsson, D. Kim, Y.-C. Yang, L. W. Smith, C. B. Simmons, D. R. Ward, R. H. Foote, J. Corrigan, D. E. Savage, M. G. Lagally, M. Friesen, S. N. Coppersmith, and M. A. Eriksson, npj Quantum Information **3**, 32 (2017).

[31] E. Jones, T. Oliphant, P. Peterson *et al.*, SciPy: Open source scientific tools for Python, http://www.scipy.org/.

[32] R. Cabrera and W. Baylis, Phys. Lett. A **368**, 25 (2007).

[33] F. A. Calderon-Vargas and J. P. Kestner, Phys. Rev. B **91**, 035301 (2015).